AIP | The Journal of Chemical Physics

The millimeter wave spectrum of silver monoxide, AgO

T. Steimle, M. Tanimoto, K. Namiki, and S. Saito

Citation: The Journal of Chemical Physics **108**, 7616 (1998); doi: 10.1063/1.476196
View online: http://dx.doi.org/10.1063/1.476196
View Table of Contents: http://scitation.aip.org/content/aip/journal/jcp/108/18?ver=pdfcov
Published by the AIP Publishing

JOURNAL OF CHEMICAL PHYSICS VOLUME 108, NUMBER 18 8 MAY 1998

The millimeter wave spectrum of silver monoxide, AgO

T. Steimle
Department of Chemistry and Biochemistry, Arizona State University, Tempe, Arizona 85287

M. Tanimoto
Department of Chemistry, Faculty of Science, Shizuoka University, Shizuoka, Japan

K. Namiki[a] and S. Saito
Institute for Molecular Sciences, Okazaki 444, Japan

(Received 5 January 1998; accepted 4 February 1998)

The pure rotational spectra of ^{107}AgO and ^{109}AgO were recorded in the 117–380 GHz spectral region using a dc-sputtering absorption cell. The ^{107}Ag$(I=1/2)$ and ^{109}Ag$(I=1/2)$ magnetic hyperfine parameters are interpreted in terms of plausible electronic configuration contributions to the $X\ ^2\Pi_i$ state. It is shown that the determined unusual sign of the Λ-doubling and Fermi contact parameters implies that the $X\ ^2\Pi_i$ state is dominated by a three open shell configuration. A comparison with isovalent CuO is made. © *1998 American Institute of Physics.* [S0021-9606(98)01618-3]

I. INTRODUCTION

Early models for bonding in the $X\ ^2\Pi_i$ ground and the low lying $A\ ^2\Sigma^+$ excited (sometimes referred to as $Y\ ^2\Sigma^+$) states of CuO and AgO (Refs. 1–5) were devoid of many of the complexities inherent in models for other transition metal compounds (e.g., multiple d-orbital bonds, π-electron back donation, etc.). The bonding was simply described as purely ionic arising from coupling of the $\mathrm{M}^+((n-1)d^{10})$ ground state configuration with the $\mathrm{O}^-(2p^5)$ electrons,

$$\mathrm{M}^+((n-1)d^{10})\mathrm{O}^-(2p^5)$$

$$\rightarrow(\mathrm{core})1\sigma^2 1\delta^4 1\pi^4 2\sigma^2 2\pi^3 \rightarrow X\ ^2\Pi_i \tag{1}$$

$$\rightarrow(\mathrm{core})1\sigma^2 1\delta^4 1\pi^4 2\sigma^1 2\pi^4 \rightarrow A\ ^2\Sigma^+, \tag{2}$$

where in labeling the molecular orbitals only the valence orbitals of M^+ and O^- have been considered. The significant excitation energy associated with ionic states arising from the open-shell $(n-1)d^9ns^1$, $(n-1)d^8ns^2$, and $(n-1)d^8ns^1np^1$ configurations (Cu$^+$: >2.8 eV and Ag$^+$: >5.0 eV) (Ref. 6) and the large ratio of radial extent of the ns to the $(n-1)d$ orbitals [Cu$^+$: ≈ 3.3 (Ref. 7) and Ag$^+$: ≈ 2.7 (Ref. 8)] was used to rationalize the prediction that these configurations were not important in describing bonding in the $X\ ^2\Pi_i$ and $A\ ^2\Sigma^+$ states. Subsequent spectroscopic observations for CuO illustrated that such a simple model was woefully inaccurate. Specifically, the optical,[9,10] infrared,[11] and microwave[12–14] spectra revealed that the ^{63}Cu$(I=3/2)$ and ^{65}Cu$(I=3/2)$ magnetic hyperfine interactions in $X\ ^2\Pi_i$ and $A\ ^2\Sigma^+$ states were large. In contrast, the configurations depicted in Eqs. (1) and (2) will result in negligible magnetic hyperfine interactions because the unpaired electron occupies the 2π or 2σ O^--centered molecular orbital. A more recent *ab initio* calculation for CuO employing extensive correlation treatment[15] confirmed that the ionic bonding resulting from coupling the open shell $(n-1)d^9ns^1$ electrons with the $\mathrm{O}^-(2p^5)$ electrons is indeed important for CuO, and presumably also important for AgO,

$$\mathrm{M}^+((n-1)d^9ns^1)\mathrm{O}^-(2p^5)$$

$$\rightarrow(\mathrm{core})1\sigma^1 1\delta^4 1\pi^4 2\sigma^2 2\pi^3 3\sigma^1$$

$$\rightarrow X\ ^2\Pi_i + (^4\Pi_i \quad \text{and} \quad ^2\Pi_r). \tag{3}$$

Furthermore, this calculation predicted a significant covalent character arising from back donation of O^- centered charge into Cu $4p\pi$ and $3d\pi$ orbitals which may also be important for AgO,

$$\mathrm{M}((n-1)d^9ns^1np^1_{\pm 1})\mathrm{O}(2p^1_0 2p^3_{\pm 1})$$

$$\rightarrow(\mathrm{core})1\sigma^1 1\delta^4 1\pi^4 2\sigma^2 2\pi^3 3\sigma^1$$

$$\rightarrow X\ ^2\Pi_i + (^4\Pi_i \quad \text{and} \quad ^2\Pi_r). \tag{4}$$

The 2π orbital of Eq. (3) is essentially a $2p_{\pm 1}$ O^--centered orbital whereas in Eq. (4) it is a bonding mixture of $2p_{\pm 1}$ O-centered and $4p_{\pm 1}$ plus $3d_{\pm 1}$ Cu-centered or $5p_{\pm 1}$ plus $4d_{\pm 1}$ Ag-centered atomic orbitals.

The heretofore lack of magnetic hyperfine interaction information has inhibited experimentally testing the proposed bonding for AgO. The fine structure parameters for the $A\ ^2\Sigma^+$ and $X\ ^2\Pi_i$ band system were derived recently[16] from the analysis of the $A\ ^2\Sigma^+ \rightarrow X\ ^2\Pi_i$ band system recorded by Fourier transform infrared (FTIR) emission spectroscopy. The analysis of the visible emission spectrum, recorded at medium resolution using a conventional spectrograph, was reported some time ago.[17] Unlike similar spectra of CuO, neither spectra exhibited magnetic hyperfine splitting. This is primarily because the ^{107}Ag$(I=1/2)$ and ^{109}Ag$(I=1/2)$ magnetic moments are approximately a factor of 20 smaller than those for ^{63}Cu$(I=3/2)$ and ^{65}Cu$(I=3/2)$. The more subtle difference in the magnetic hyperfine interaction between the two molecules reflects the periodic trend in bonding and is

---

[a] Present address: Department of Chemistry and Biochemistry, Arizona State University, Tempe, Arizona 85287.

the focus of the present study. Although it is expected that the ionic bonding contribution for AgO and CuO should be comparable because of the similar ionization potential of Cu and Ag, the degree of mixing between the $(n-1)d^{10}$ and $(n-1)d^9ns^1$ asymptotes in the description of this ionic bond should be significantly different. Specifically, the mixing should be much less important for AgO than for CuO because the $^1S((n-1)d^{10})$–$^3D((n-1)d^9ns^1)$ separation for Ag^+ ($\approx$5.0 eV) is much larger than for Cu^+ ($\approx$1.5 eV). Furthermore the energy disparity between the $5p_{\pm 1}$ of Ag^+ orbital and the O^- valence orbitals in comparison to the $4p_{\pm 1}$ of Cu^+ will hinder the covalent bonding arising from backdonation. These qualitative differences in the bonding of CuO and AgO are in accord with the conclusions of the recent *ab initio* prediction.[18] Here we report on the analysis of the mm-wave absorption of both the ^{107}AgO and ^{109}AgO isotopomers and the interpretation of the magnetic hyperfine interactions and Λ-doubling effects.

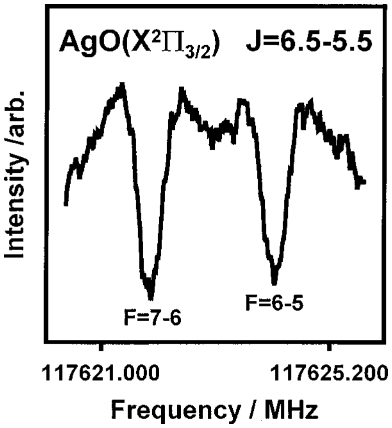

FIG. 1. The recorded mm-wave spectrum associated with the $J=6.5\leftarrow J=5.5$ pure rotational transition of the $X\ ^2\Pi_{3/2}$ subband for ^{107}AgO. The splitting is caused by the ^{107}Ag ($I=1/2$) magnetic hyperfine interaction. The e-parity and f-parity spectral features are not resolved.

II. EXPERIMENT

All measurements were performed at the Institute for Molecular Science using a long path absorption cell apparatus similar to that used in the recent study of CuO.[14] The experimental set up has been described previously.[19,20] Silver monoxide was produced in 2 m long free space flowing absorption cell by dc-sputtering of a cylindrical silver foil inserted in the cathode. A 3:1 mixture of helium and O_2 was slowly flowed through the cell and a discharge current of approximately 500 mA was maintained. The absorption cell was cooled to a temperature of -170 °C by flowing liquid nitrogen through a copper tube attached to a copper sheet covering the Pyrex absorption cell. It is estimated that the pressure in the absorption cell was $\approx$10 mTorr. The tunable microwave radiation was derived from harmonic generation of free running klystrons operating in the 65–120 GHz range. The radiation was frequency modulated at 50 kHz and a liquid He cooled InSb detector signal processed at 100 kHz with a lock-in amplifier. The Earth's magnetic field was compensated by adjusting currents through a solenoid coil around the cell and a pair of Helmholtz coils placed perpendicular to the cell.

III. OBSERVATIONS AND ANALYSIS

A total of 44 and 45 spectral features associated with the pure rotational transitions from $J=6.5\leftarrow J=5.5$ to $J=20.5\leftarrow J=19.5$ in the 117 GHz to 370 GHz frequency range for the ^{107}AgO and ^{109}AgO isotopomers, respectively, were measured. The results from the analysis of the $A\ ^2\Sigma^+\rightarrow X\ ^2\Pi_i$ band system was of the great assistance[16] in assigning the observed mm-wave spectrum. The recorded spectrum associated with the $J=6.5\leftarrow J=5.5$ pure rotational transition of the $X\ ^2\Pi_{3/2}$ subband is illustrated in Fig. 1. This spectrum was recorded using a 1 ms time constant on the lock-in amplifier, a pressure of approximately 50 mTorr and a temperature of -170 °C. The spectrum represents an average of 200 scans. The 500 kHz (FWHM) linewidth is mainly due to pressure broadening and to a lesser extent Zeeman effects.

The Λ-doubling and the hyperfine effects on all of the measured transitions in the $X\ ^2\Pi_{3/2}$ subband are small. Therefore, each rotational transition for this subband consists, in principle, of four closely spaced spectral features associated with the strongly allowed $\Delta F=\Delta J=+1$ transitions, two hyperfine components associated with the e-parity levels and two associated with f-parity levels of the Λ-doublet. At low-J the Λ-doubling effects in the $X\ ^2\Pi_{3/2}$ subband are negligible and e-parity and f-parity spectral features are not resolved as illustrated in Fig. 1. The splitting of the spectral features caused by the Λ-doubling increases approximately linearly with J whereas the hyperfine interaction contribution decreases nonlinearly with J. The net effect is that with increasing J the spectral pattern changes from the two features illustrated in Fig. 1 into four overlapped features which then rapidly coalesce back to two features. The Λ-doubling effects on the measured pure rotational transitions in the $X\ ^2\Pi_{1/2}$ subband are very large and well resolved for all the observed transitions. The transitions associated with low-J $X\ ^2\Pi_{1/2}$ subband exhibit a small magnetic hyperfine splitting of similar magnitude to those of the $X\ ^2\Pi_{3/2}$ subband. Unlike CuO, there is no measurable difference between the observed magnetic hyperfine splitting of the spectral features associated with the e-parity and f-parity levels in the $X\ ^2\Pi_{1/2}$ subband indicating that the parity dependent magnetic hyperfine doubling term is negligible (see below). The total angular momentum quantum number, F, assignment for the hyperfine split component of the low-J spectral features was based upon relative intensity considerations. The assignment, observed frequencies and the difference between observed and calculated frequencies are given in Table I. Like CuO the $X\ ^2\Pi_{1/2}$ subband transitions were detected at a frequency lower than that of the $X\ ^2\Pi_{3/2}$ subband transitions (see Table I) indicating that the $B^{\mathrm{eff}}(X\ ^2\Pi_{1/2}) < B^{\mathrm{eff}}(X\ ^2\Pi_{3/2})$ which is abnormal for an inverted $^2\Pi$ state. This is due to an unusually large value for A_D.

The analysis was similar to that performed for CuO.[14] The effective Hamiltonian operator used to model the system was

TABLE I. Observed transition frequencies for ^{107}AgO and ^{109}AgO (in MHz).

J'', F''[a]	$\nu(1/2,f)$[b]	$\Delta\nu$[c]	$\nu(1/2,e)$[b]	$\Delta\nu$[c]	$\nu(3/2,f)$[b]	$\Delta\nu$[c]	$\nu(3/2,e)$[b]	$\Delta\nu$[c]
^{107}AgO								
4.5, 5					99 529.460[d]			−0.007
5.5, 5	117 67.624	−0.001			117 624.354[d]			0.017
5.5, 6	117 168.704	−0.004			117 622.056[d]			0.021
6.5, 6	135 201.580	−0.005	135 377.514	0.018	135 713.971[d]			−0.003
6.5, 7	135 202.362	0.018	135 378.256	0.000	135 712.306[d]			0.001
8.5, 8	171 261.806	−0.024	171 437.246	−0.015	171 885.767[d]			−0.012
8.5, 9					171 884.756[d,e]			−0.063
10.5	207 309.220	0.029	207 484.009	−0.019	208 044.801[d]			−0.035
13.5	261 351.056	−0.017	261 524.824	0.015	262 255.276	−0.041	262 254.035	0.039
14.5	279 355.947	0.006	279 529.264	0.011	280 316.146	0.000	280 314.566[e]	−0.071
15.5	297 355.703	−0.010	297 528.565	−0.008	298 371.835	0.011	298 370.143	0.030
16.5	315 350.057	−0.003	315 522.443	0.003	316 422.012	−0.005	316 420.066	−0.026
17.5	333 338.677	0.026	333 510.532	0.008	334 466.438	0.044	334 464.215	−0.026
18.5	351 321.140	−0.018	351 492.475	−0.019	352 504.708[e]	0.088	352 502.251	0.023
19.5	369 297.254	0.004	369 468.030	0.007	370 536.350	−0.014	370 533.704	−0.015
	rms=0.022							
^{109}AgO								
4.5, 4					99 295.966[d]			−0.031
4.5, 5					99 292.177[d]			−0.003
5.5, 5			117 063.560	0.030	117 344.372[d]			0.010
5.5, 6			117 064.760	−0.021	117 341.731[d]			0.011
6.5, 6	134 878.762	−0.021	135 054.255	−0.033	135 390.873[d]			0.005
6.5, 7	134 879.655	−0.006	135 055.194	0.029	135 388.931[d]			−0.021
8.5, 8	170 853.090	0.028	171 028.077	−0.008	171 476.538[d]			0.038
8.5, 9					171 475.372[d]			−0.027
10.5	206 814.434	−0.015	206 988.867	−0.012	207 549.334[d,e]			−0.099
13.5	260 727.506	−0.003	260 900.823	−0.014	261 631.038	0.021	261 629.610	−0.030
14.5	278 689.468	−0.010	278 862.385	0.002	279 648.881	−0.040	279 647.378	0.031
15.5	296 646.413	0.037	296 818.861	0.032	297 661.570[e]	−0.130	297 659.977[e]	0.062
16.5	314 597.869	−0.005	314 769.846	−0.002	315 669.060	0.039	315 667.032	0.018
17.5	332 543.651	0.007	332 715.119	0.010	333 670.550	−0.006	333 668.292	−0.019
18.5	350 483.346	−0.012	350 654.277	−0.010	351 665.963	0.008	351 663.496	0.020
19.5	368 416.681	−0.006	368 587.047	−0.006	369 654.932	−0.003	369 652.160	−0.018
	rms=0.023							

[a] Quantum numbers of the lower level for the transition, $(J''+1,F''+1)\leftarrow(J'',F'')$.

[b] The hyperfine splitting is not resolved for transitions associated with $J''\geqslant 8.5$ in the $^2\Pi_{1/2}$ sublevel and $J''\geqslant 10.5$ in the $^2\Pi_{3/2}$ sublevel. The observed spectral feature is assigned to the mean of the two strongly allowed $(\Delta F=\Delta J=+1)$ hyperfine components.

[c] The deference between observed and calculated frequencies, $\Delta\nu=\nu_{\text{obs.}}-\nu_{\text{calc.}}$.

[d] The Λ-doubling is not resolved for transitions associated with $J''<8.5$ in the $^2\Pi_{3/2}$ sublevel. The observed spectral feature is assigned to the mean of the two strongly allowed $(\Delta F=\Delta J=+1)$ Λ-doublets.

[e] Not included in the least-squares fitting.

$$\mathbf{H}^{\text{eff}}=\mathbf{H}^{\text{so}}+\mathbf{H}^{\text{rot}}+\mathbf{H}^{\text{ld}}+\mathbf{H}^{\text{mhf}}. \tag{5}$$

Expressions for the spin–orbit, $\mathbf{H}^{\text{so}}$, rotational, $\mathbf{H}^{\text{rot}}$, and Λ-doubling, $\mathbf{H}^{\text{ld}}$, terms are readily available in the literature.[21–23] The magnetic hyperfine operator, $\mathbf{H}^{\text{mhf}}$, is given by[24–27]

$$\begin{aligned}\mathbf{H}^{\text{mhf}}=&\,aI_zL_z+b_F\mathbf{I}\cdot\mathbf{S}+c[I_zS_z-\tfrac{1}{3}\mathbf{I}\cdot\mathbf{S}]\\&+\tfrac{1}{2}d[e^{2i\phi}I_-S_-+e^{-2i\phi}I_+S_+].\end{aligned} \tag{6}$$

In Eq. (6) **I** and **S** are the nuclear and electron spin angular momentum operators, respectively. The data set consisted of transitions associated with high J levels making centrifugal distortion corrections necessary. The eigenvectors and eigenvalues for the $X\,^2\Pi_i$ state were obtained by constructing and diagonalizing a $4\times 4(=(2S+1)(2I+1)\times(2S+1)(2I+1))$ matrix representation in a *case* $a_{\beta J}$ basis set. The matrix elements for the $\mathbf{N}^2$ operator form given by Amoit *et al.*[28] were used to facilitate a comparison with the results of the FTIR studies. The spin–orbit parameter, A, was held fixed to the value determined from FTIR electronic emission spectroscopy.[16]

The hyperfine splitting is not resolved for transitions associated with $J''\geqslant 8.5$ in the $^2\Pi_{1/2}$ sublevel and $J''\geqslant 10.5$ in the $^2\Pi_{3/2}$ sublevel. In those cases the observed spectral feature is assigned to the intensity weighted mean of the two strongly allowed $(\Delta F=\Delta J=+1)$ hyperfine components. The Λ-doubling is not resolved for transitions associated with $J''<10.5$ in the $^2\Pi_{3/2}$ sublevel. In those cases the observed spectral feature is assigned to the intensity weighted mean of the two strongly allowed $(\Delta F=\Delta J=+1)$ Λ-doublets. Attempts to model the data with various combinations of the magnetic hyperfine parameters were made. The Λ-doubling type magnetic hyperfine parameter, d, was constrained to zero because there was no measurable differ-

TABLE II. Spectroscopic parameters for the $X\ ^2\Pi_i$ state of AgO (in MHz).[a]

	^{107}AgO		^{109}AgO	
Parameters[a]	mm-wave	FTIR[b]	mm-wave	FTIR[b]
B	9 035.497 1(59)	9 034.79(55)	9 013.971 3(55)	9 013.95(56)
D	0.013 800 91(113)	0.013 754(162)	0.013 7.34 14(101)	0.013 9.70(186)
A	−8 073 882[c]	−8 073 882(49)	−8 073 915[c]	−8 073 915(56)
A_D	48.144 99(142)	48.360(90)	48.029 79(136)	48.443(132)
A_H	−0.000 100 80(149)		−0.000 098 32(140)	
γ_D		−0.062 4(113)		−0.091 4(198)
p	−175.667(37)	−171.8(26)	−175.216(34)	−182.2(29)
p_D	0.006 848(53)	0.005 19(132)	0.006 892(50)	0.009 14(144)
q	−1.039 9(119)	−0.91(36)	−1.082 1(109)	−0.79(41)
h_1[d]	−108.4(114)		−109.8(77)	
h_2	69.9(36)		75.7(21)	
h_3	206(101)		93(65)	

[a] The number in parentheses represent two standard deviation error in the last quoted figure.

[b] Reference 16.

[c] Held fixed to the FTIR value.

[d] $h_1 \equiv a - \frac{1}{2}(b_F + 2c/3)$, $h_2 \equiv a + \frac{1}{2}(b_F + 2c/3)$, and $h_3 \equiv b_F - c/3$.

ence between the observed magnetic hyperfine splitting of the spectral features associated with the e-parity and f-parity levels in the $X\ ^2\Pi_{1/2}$ subband. The three optimized magnetic hyperfine fitting parameters were taken as the linear combinations $h_1 \equiv a - \frac{1}{2}(b_F + 2c/3)$, $h_2 \equiv a + \frac{1}{2}(b_F + 2c/3)$, and $h_3 \equiv b_F - c/3$($\equiv$Frosch and Foley b). The parameters h_1 and h_2 are directly proportional to the $^2\Pi_{1/2}$ and $^2\Pi_{3/2}$ diagonal matrix elements in a *case* $a_{\beta J}$ basis set and are well determined. The parameter h_3 is associated with only off-diagonal elements and accordingly is not well determined because the energy level pattern of AgO ($X\ ^2\Pi$) is that of a nearly pure *case* $a_{\beta J}$ molecule. The optimized parameters and associated errors produced from a nonlinear least squares fitting procedure are presented in Table II along with those from Ref. 16 for comparison. Although the rms of 22 kHz and 23 kHz for the ^{107}AgO and ^{109}AgO data sets, respectively, suggest that the fitting model is adequate, there is a slight deficiency in the region where the hyperfine splitting is comparable to the Λ-doubling. Specifically, the two Λ-doublets for the $J=9.5 \leftarrow J=8.5$ rotational transition of the $^2\Pi_{3/2}$ sublevel are predicted to be separated by approximately 600 kHz, yet the observed spectral feature has a line width of approximately 800 kHz and is not severely distorted. Furthermore, three features were omitted from the fit (see Table I) because their deviation from the calculated value was slightly larger than the estimated precision of 60 kHz.

IV. DISCUSSION

A. Fine structure parameters

The primary objective of this study is to determine the significance of the three open shell configurations of Eqs. (3) and (4) in describing the $X\ ^2\Pi_i$ state of AgO and to make a comparison with CuO. It will now be shown that both the sign and magnitude of the Λ-doubling and the magnetic hyperfine parameters are consistent with assuming that the three open shell configurations makes a significant, if not dominant, contribution to the $X\ ^2\Pi_i$ state. This is inconsistent with the current theoretical predictions for AgO.[18]

The mm-wave spectrum could be equally well reduced to Λ-doubling fitting parameters $(p+2q)$ and q of either sign depending upon the assignment. These parameters are dominated by second order contributions, which assuming the unique perturber, identical potential approximations are[29]

$$p = 4\,\frac{\langle (X^2\Pi_i(\Lambda=+1,\Sigma=-\tfrac{1}{2})|\,\dfrac{\hbar^2}{2\mu R^2}\,L^+|A^2\Sigma^+_{\frac{1}{2}}(\Sigma=-\tfrac{1}{2})\rangle\langle X^2\Pi_{\frac{1}{2}}(\Lambda=+1,\Sigma=-\tfrac{1}{2})|\Sigma_i a_i \tfrac{1}{2}(l_i^+ s_i^-)|A^2\Sigma^+_{\frac{1}{2}}(\Sigma=+\tfrac{1}{2})\rangle}{E(X\ ^2\Pi_i)-E(A\ ^2\Sigma^+)}, \qquad (7)$$

$$q = 2\,\frac{|\langle X\ ^2\Pi_i(\Lambda=+1,\Sigma=-\tfrac{1}{2})|\,\dfrac{\hbar^2}{2\mu R^2}\,L^+|A^2\Sigma^+_{\frac{1}{2}}(\Sigma=-\tfrac{1}{2})\rangle|^2}{E(X\ ^2\Pi_i)-E(A\ ^2\Sigma^+)}\,. \qquad (8)$$

A sign for $(p+2q)$ consistent with that determined from the FTIR analysis,[16] but opposite to that determined for CuO (Ref. 30) and that implied by the theoretical prediction,[18] was used. The negative sign determined for $(p+2q)$ from the FTIR analysis is based upon assuming a Σ^+ symmetry for the excited electronic state associated with the observed band system. Such an assumption is consistent with the observed intensities and with the theoretical prediction[18] for the energy separation between the $X\ ^2\Pi_i$ and $A\ ^2\Sigma^+$ states. If it is assumed that $X\ ^2\Pi_i$ and $A\ ^2\Sigma^+$ states are dominated by the configurations of Eqs. (1) and (2) (i.e., a hole in the $2p$-orbital centered on O^-) then the matrix elements in Eqs. (7) and (8) can be approximated as

$$\langle X\ ^2\Pi_i(\Lambda=+1,\Sigma=-\tfrac{1}{2})|\frac{\hbar^2}{2\mu R^2}L^+|A^2\Sigma^+_{\frac{1}{2}}(\Sigma=-\tfrac{1}{2})\rangle$$

$$=B\cdot\langle 2\sigma|l^+|2\pi\rangle\approx -B\sqrt{2} \tag{9}$$

and

$$\langle X\ ^2\Pi_{\frac{1}{2}}(\Lambda=+1,\Sigma=-\tfrac{1}{2})|\Sigma_i a_i\tfrac{1}{2}(l_i^+s_i^-)|A^2\Sigma^+_{\frac{1}{2}}(\Sigma=+\tfrac{1}{2})\rangle$$

$$=\langle 2\sigma|\tfrac{1}{2}a(l^+s^-)|2\pi\rangle\approx\tfrac{1}{2}a_\pi\sqrt{2}, \tag{10}$$

where $a_\pi\equiv\langle 2\pi|al_z|2\pi\rangle$ and B is the rotational constant. Substitution into Eqs. (7) and (8) give the commonly used approximate expressions[29]

$$p=\frac{4B_\nu A}{E(X\ ^2\Pi_i)-E(A\ ^2\Sigma^+)}, \tag{11}$$

$$q=\frac{4B_\nu^2}{E(X\ ^2\Pi_i)-E(A\ ^2\Sigma^+)}, \tag{12}$$

where A is the spin–orbit parameter. As noted in the analysis of the FTIR spectra,[16] expression (12) predicts that the Λ-doubling fitting parameter $(p+2q)$ should be positive for AgO, contrary to observation. The predicted sign of the Λ-doubling fitting parameters q is consistent with observation.

Expressions analogous to Eqs. (11) and (12) for states arising from the three open shell configurations of Eqs. (3) and (4) are readily derived. The spin adapted wave functions for the inverted $^2\Pi_i(\Omega=+\frac{1}{2})$ substate arising from these configurations is[31]

$$\Psi(^2\Pi_i(\Omega=+\tfrac{1}{2}))=\frac{1}{\sqrt{6}}(2|1\overline{\sigma}2\pi^+2\overline{\pi}^+2\overline{\pi}^-3\sigma2\sigma2\overline{\sigma}|$$

$$-|1\overline{\sigma}2\pi^+2\overline{\pi}^+2\overline{\pi}^-3\overline{\sigma}2\sigma2\overline{\sigma}|$$

$$-|1\sigma2\pi^+2\overline{\pi}^+2\overline{\pi}^-3\overline{\sigma}2\sigma2\overline{\sigma}|). \tag{13}$$

The ‘‘$\overline{\ }$’’ over the orbital indicates a β spin function. The spin adapted wave function for two $^2\Sigma^+$ states arising from the configuration associated with the promotion of an electron from the 2σ orbital to a 2π orbital are

$$\Psi(^2\Sigma(\Omega=+\tfrac{1}{2}))=\frac{1}{\sqrt{2}}(|1\sigma2\pi^+2\overline{\pi}^+2\overline{\pi}^-3\overline{\sigma}2\sigma2\pi^-|$$

$$-|1\overline{\sigma}2\pi^+2\overline{\pi}^+2\overline{\pi}^-3\sigma2\sigma2\pi^-|), \tag{14}$$

$$\Psi(^2\Sigma^+(\Omega=+\tfrac{1}{2}))$$

$$=\frac{1}{\sqrt{6}}(2|1\sigma2\pi^+2\overline{\pi}^+2\overline{\pi}^-3\sigma2\overline{\sigma}2\pi^-|$$

$$-|1\sigma2\pi^+2\overline{\pi}^+2\overline{\pi}^-3\overline{\sigma}2\sigma2\pi^-|$$

$$-|1\overline{\sigma}2\pi^+2\overline{\pi}^+2\overline{\pi}^-3\sigma2\sigma2\pi^-|). \tag{15}$$

The wave functions for the two $^2\Sigma^+(\Omega=-\frac{1}{2})$ states are simply derived by interchanging the α and β spin functions on the unfilled orbitals. Using these spin adapted functions and the rules for evaluating the matrix elements between Slater determinants[32] the unique perturber, pure precession, identical potential, expressions become

$$p=\frac{-3BA}{E(^2\Pi_i)-E(^2\Sigma^+(\text{Eq. }14))}, \tag{16}$$

$$p=\frac{\frac{1}{3}BA}{E(^2\Pi_i)-E(^2\Sigma^+(\text{Eq. }15))}, \tag{17}$$

$$q=\frac{3B^2}{E(^2\Pi_i)-E(^2\Sigma^+(\text{Eq. }14))}, \tag{18}$$

$$q=\frac{B^2}{E(^2\Pi_i)-E(^2\Sigma^+(\text{Eq. }15))}. \tag{19}$$

Thus it can be seen from Eqs. (16)–(19) that the negative values for the Λ-doubling fitting parameters $(p+2q)$ and q are consistent with the three unpaired configuration. Using the values of the A and B values of the $X\ ^2\Pi_i$ state and $\Delta E_{\Pi\Sigma}$ from the FTIR analysis $(=-8294\ \text{cm}^{-1})$,[16] and assuming that the wave function for the $A\ ^2\Sigma^+$ is given by Eq. (14) gives $(p+2q)=-870$ MHz and $q=-4.8$ MHz. This simple prediction gives the correct sign for the Λ-doubling parameters, but magnitudes that are approximately a factor of 4 too large. The implemented ‘‘identical potential’’ assumption, which implies a vibrational overlap integral of unity, will force the model to over estimate the interaction between the $X\ ^2\Pi_i$ and $A\ ^2\Sigma^+$ states. A more reasonable estimate for the magnitude of the vibrational overlap integral is between 0.70 and 0.30 given that $\Delta v\neq 0$ transitions in the $A\ ^2\Sigma^+\rightarrow X\ ^2\Pi_i$ band system were observed and that the difference in bond distances for the two states is approximately 0.07 Å.[16] Thus the Λ-doubling parameters indicate that the $X\ ^2\Pi_i$ state is dominated by the three open shell configurations.

A comment on the unusually large centrifugal distortion to the spin–orbit parameter, A_D, is warranted. This ‘‘effective’’ parameter also has contributions from the spin–rotation interaction, γ. The values for A_D for the two isotopes are almost exactly in the ratio of their inverse reduced mass. This implies that the contribution from the spin–rotation interaction is negligible.

TABLE III. The Ag and Cu atomic information used to estimate the magnetic hyperfine parameters.

	^{107}Ag	^{109}AgO	^{63}Cu
g_I	$-0.227\,14$ [a]	$-0.261\,38$ [a]	$1.482\,2$ [a]
$\langle ns\vert\delta(r)\vert ns\rangle$	6.36×10^{31} m^{-3} [b]	6.38×10^{31} m^{-3} [b]	3.334×10^{31} m^{-3} [e]
$\langle nd\vert r^{-3}\vert nd\rangle$	5.71×10^{31} m^{-3} [c]	5.72×10^{31} m^{-3} [c]	2.4×10^{31} m^{-3} [e]
$\langle (n-1)p\vert r^{-3}\vert (n-1)p\rangle$	⋯	2.12×10^{31} m^{-3} [d]	0.53×10^{31} m^{-3} [e]
$\langle p_{\pm1}\vert(3\cos^2\Theta-1)\vert p_{\pm}\rangle$	$-2/5$	$-2/5$	$-2/5$
$\langle p_{\pm1}\vert\sin^2\Theta\vert p_{\pm1}\rangle$	4/5	4/5	4/5
$\langle d_0\vert(3\cos^2\Theta-1)\vert d_0\rangle$	4/7	4/7	4/7
$\langle d_{\pm1}\vert(3\cos^2\Theta-1)\vert d_{\pm1}\rangle$	2/7	2/7	2/7
$\langle d_{\pm1}\vert\sin^2\Theta\vert d_{\pm1}\rangle$	4/7	4/7	4/7

[a] Reference 35.
[b] Reference 33.
[c] Reference 32.
[d] Reference 34.
[e] Reference 36.

B. Hyperfine structure parameters

The magnetic hyperfine parameters are extremely sensitive to the nature of the electronic wave function. Atomic information and the assumed nature of the open shell 1σ, 2π, and 3σ orbitals will be used to estimate the hyperfine parameters as a test of the proposition that the three open shell configuration is important in describing the $X\ ^2\Pi_i$ state. The three open shell orbitals are approximated as are linear combinations of the $4d$, $5s$, and $5p$ Ag atomic and the $2p$ O atomic orbitals,

$$\psi(1\sigma)\approx 4d_0(\mathrm{Ag}), \tag{20}$$

$$\psi(3\sigma)\approx 5s(\mathrm{Ag}) \tag{21}$$

$$\psi(2\pi)\approx c_1 2p_{\pm1}(\mathrm{O})+c_2 4d_{\pm1}(\mathrm{Ag})+c_3 5p_{\pm1}(\mathrm{Ag}). \tag{22}$$

Using the rules for calculating the matrix elements involving Slater determinants[32] the predicted hyperfine parameters associated with the wave function of Eq. (13) are

$$a/\mathrm{Hz}=1.4137\times10^{-23}\ \mathrm{m}^3\ \mathrm{s}^{-1}\ g_I\langle 2\pi|r^{-3}|2\pi\rangle, \tag{23}$$

$$b_F/\mathrm{Hz}=1.1843\times10^{-22}\ \mathrm{m}^3\ \mathrm{s}^{-1}\ g_I(-\tfrac{1}{3})\langle 3\sigma|\delta(r)|3\sigma\rangle, \tag{24}$$

$$\begin{aligned} c/\mathrm{Hz}=2.123\times10^{-23}\ \mathrm{m}^3\ \mathrm{s}^{-1}\ g_I(\tfrac{2}{3}) &\times\left[\langle 2\pi|\left(\frac{3\cos^2\Theta-1}{r^{-3}}\right)|2\pi\rangle\right.\\ &\left.+\langle 1\sigma|\left(\frac{3\cos^2\Theta-1}{r^{-3}}\right)|1\sigma\rangle\right], \end{aligned} \tag{25}$$

$$d/\mathrm{Hz}=2.143\times10^{-23}\ \mathrm{m}^3\ \mathrm{s}^{-1}\ g_I(\tfrac{2}{3})\langle 2\pi|\frac{\sin^2\Theta}{r^{-3}}|2\pi\rangle. \tag{26}$$

The 3σ orbital contributes only to b_F, the 2π orbital contributes only to a and d, whereas both the 2π and 1σ orbitals contribute to c. In this analysis the use of the experimental information for the neutral atom, Ag, for the estimating the expectation values in Eqs. (23)–(26) is necessitated because of the lack of such information for the ion, Ag$^+$. The appropriate atomic expectation values[33–36] and atomic g_I values[37] for ^{107}Ag, ^{109}Ag, and ^{63}Cu are given in Table III. The theoretical prediction[18] gives no information from which the coefficients c_1–c_3 of Eq. (22) can be estimated. The predicted magnetic hyperfine parameters for the three limiting cases (i.e., $c_1=1$, $c_2=c_3=0$, etc.) are collected in Table IV.

TABLE IV. Estimated magnetic hyperfine parameters for AgO($X\ ^2\Pi_i$) (in MHz).[a]

	^{107}AgO			^{109}AgO		
	$2\pi\approx 2p_{\pm1}$ [b]	$2\pi\approx 4d_{\pm1}$ [c]	$2\pi\approx 5p_{\pm1}$ [d]	$2\pi\approx 2p_{\pm1}$ [b]	$2\pi\approx 4d_{\pm1}$ [c]	$2\pi\approx 5p_{\pm1}$ [d]
a	0	-183	-68	0	-211	-78
b_F	571	571	571	655	655	655
c	-104	-78	-157	-120	-89	-180
d	0	105	-55	0	120	-63
$a+\frac{1}{2}(b_F+2c/3)$	250	77	165	288	86	190
$a-\frac{1}{2}(b_F+2c/3)$	-250	-442	-301	-288	-510	-346
$b_F-c/3$	605	597	623	695	684	715

[a] Calculated using Eqs. (23)–(26) and data of Table III.
[b] Calculated assuming $c_1=1$, $c_2=0$, and $c_3=0$ in Eq. (22).
[c] Calculated assuming $c_1=0$, $c_2=1$, and $c_3=0$ in Eq. (22).
[d] Calculated assuming $c_1=0$, $c_2=0$, and $c_3=1$ in Eq. (22).

It is satisfying that the determined sign for fitting parameters of h_1, h_2 and h_3 are consistent with the values predicted for the proposed three open-shell configuration given in Table IV. Furthermore it is noted that the ratio $h_i(^{107}\mathrm{AgO})/h_i(^{109}\mathrm{AgO})$ is $=g_I(^{107}\mathrm{AgO})/g_I(^{109}\mathrm{AgO})$ within the experimental error indicating that the model is not merely phenomenological. The combination h_1+h_2 indicates that $a \approx -20$ MHz. The determined small value for a, and the observation that d is negligible, indicates that the 2π orbital is essentially a $2p_{\pm 1}$ O^--centered orbital with little backdonation from O^- centered charge into Ag $5p\pi$ and/or $4d\pi$ orbitals. A much more significant contribution from back donation of O electrons into Cu $4p\pi$ and $3d\pi$ orbitals was required to explain the determined hyperfine parameters for CuO.[14] This observation is consistent with the trend in the $^1S((n-1)d^{10})-^3D((n-1)d^9ns^1)$ separation for Ag^+ ($\approx$5.0 eV) and Cu ($\approx$1.5 eV). The comparison of the spin–orbit parameter of AgO with O^- (Ref. 16), was previously used to also argue that the 2π orbital is essentially a $2p_{\pm 1}$ O^--centered orbital. Therefore, a comparison of the determined parameters with those predicted under the assumption $c_1=1$, $c_2=c_3=0$ (i.e., the first column of Table IV) is most appropriate. The most striking observation from this comparison (i.e., obs. $|h_1| \approx |h_2| \approx 90$ MHz; calc: $|h_1| = |h_2| = 250$ MHz) is the implied relatively large contribution of the three open shell configurations given in Eqs. (3) and (4). This comparison suggest that the three open shell configuration is nearly as important as the singly unpaired electron configuration. Finally, although not well determined the combination of h_1, h_2, and h_3 gives a value for c of ≈ -28 MHz. A comparison with the predicted value of -104 MHz (see column 1 of Table IV) also suggest a similar contribution from the three open shell configurations to the description of the $X\ ^2\Pi_i$ state as did the comparison of the predicted observed values for $|h_1|$ and $|h_2|$.

V. CONCLUSION

The fine and hyperfine interactions in the $X\ ^2\Pi_1$ state of AgO have been analyzed. The unusual sign of the Λ-doubling and magnetic hyperfine fitting parameters can be rationalized if it is assumed that a three unpaired electron configuration makes a significant if not dominant contribution. These results imply that the excited metal ionic configuration $\mathrm{M}^+((n-1)d^9ns^1)$ is more important in AgO than in CuO even though the $^1S((n-1)d^{10})-^3D((n-1)d^9ns^1)$ separation for Ag^+ ($\approx$5.0 eV) is much larger than for Cu^+ ($\approx$1.5 eV). These observations are not in qualitative agreement with the recent *ab initio* prediction for the nature of the $X\ ^2\Pi_i$ state.

The determination of the complete set of magnetic hyperfine parameters for the $X\ ^2\Pi_i$ state would be helpful for further elucidating bonding. The parameters provided in the present study should facilitate any future FT-microwave measurements from which those parameters could be derived.

ACKNOWLEDGMENTS

The work at ASU was supported by a grant from Science Foundation-Experimental Physical Chemistry (CHE-9710174), and Grant-in-Aid of Ministry of Education, Science and Culture (No. 04233107). The authors would like to thank Professor Leah O'Brien for her helpful comments.

[1] D. H. W. Den Boer and E. W. Kaleveld, Chem. Phys. Lett. **69**, 389 (1980).

[2] P. S. Bagus, C. J. Nelin, and C. W. Bauschlicher, J. Chem. Phys. **79**, 2975 (1983).

[3] J. Schamps, B. Pinchemel, Y. Lefebvre, and G. Raseev, J. Mol. Spectrosc. **101**, 344 (1983).

[4] G. Igel, U. Wedig, M. Dolg, P. Fuentealba, H. Preuss, H. Stoll, and R. Frey, J. Chem. Phys. **81**, 2737 (1984).

[5] P. J. Hay and R. L. Martin, J. Chem. Phys. **83**, 5174 (1985).

[6] C. E. Moore, *Atomic Energy Levels*, Natl. Bur. Stand. (U.S.) Circ. No. 467 (U.S. GPO, Washington, D.C., 1949).

[7] C. W. Bauschlicher, Jr., S. P. Walch, and H. Partridge, J. Chem. Phys. **76**, 1033 (1982).

[8] C. Froese-Fischer, *The Hartree–Fock Methods for Atoms: A Numerical Approach* (Wiley, New York, 1977).

[9] O. Appelblad, I. Renhorn, M. Dulick, M. R. Purnell, and J. M. Brown, Phys. Scr. **28**, 539 (1983).

[10] T. Steimle and Y. Azuma, J. Mol. Spectrosc. **118**, 237 (1986).

[11] L. C. O'Brien, R. L. Kubicek, S. J. Wall, D. E. Koch, R. J. Friend and C. R. Brazier, J. Mol. Spectrosc. **180**, 365 (1996).

[12] M. C. L. Gerry, A. J. Merer, U. Sassenberg, and T. C. Steimle, J. Chem. Phys. **86**, 4754 (1987).

[13] T. C. Steimle, W.-L. Chang, and D. Nachman, Chem. Phys. Lett. **153**, 534 (1988).

[14] T. Steimle, K. Namiki, and S. Saito, J. Chem. Phys. (to be published).

[15] S. R. Langhoff and C. W. Bauschlicher, Chem. Phys. Lett. **124**, 241 (1986).

[16] L. C. O'Brien, S. J. Wall, and M. K. Sieber, J. Mol. Spectrosc. **183**, 57 (1997).

[17] M. J. Griffiths and R. F. Barrow, J. Phys. B **10**, 925 (1977).

[18] C. W. Bauschlicher, Jr., H. Partridge, and S. R. Langhoff, Chem. Phys. **148**, 57 (1990).

[19] S. Saito and M. Goto, Astrophys. J. **410**, L53 (1993).

[20] K. Namiki and S. Saito, Chem. Phys. Lett. **252**, 343 (1996).

[21] E. Hirota, *High-Resolution Spectroscopy of Transient Molecules*, Springer Series in Chemical Physics (Springer, Berlin, 1985).

[22] J. M. Brown, M. Kaise, C. M. L. Kerr, and D. J. Milton, Mol. Phys. **36**, 553 (1978).

[23] J. M. Brown and A. J. Merer, J. Mol. Spectrosc. **74**, 488 (1979).

[24] R. A. Frosch and H. M. Foley, Phys. Rev. **88**, 1337 (1952).

[25] G. C. Dousmanis, Phys. Rev. **97**, 967 (1955).

[26] P. Kristiansen and L. Veseth, J. Chem. Phys. **84**, 6336 (1986).

[27] C.H. Townes and A.L. Schawlow, *Microwave Spectroscopy* (Dover, New York, 1975).

[28] C. Amoit, J. P. Maillard, and C. Chauville, J. Mol. Spectrosc. **87**, 196 (1982).

[29] H. Lefebvre-Brion and R. W. Field, *Perturbations in Diatomic Molecules* (Academic, Orlando, 1986).

[30] Y. Lefebvre, B. Pinchemel, J. M. Delaval, and J. Schamps, Phys. Scr. **25**, 344 (1981).

[31] W. G. Richards and D. L. Cooper, *Ab Initio Molecular Orbital Calculations for the Chemist* (Clarendon, Oxford, 1983).

[32] M. Weissbluth, *Atoms and Molecules* (Academic, New York, 1978).

[33] A. G. Blachman, D. A. Landman, and A. Lurio, Phys. Rev. **150**, 59 (1966).

[34] H. Dahmen and S. Penselin, Z. Phys. **200**, 456 (1967).

[35] W. Fischer, H. Hühnermann, and E. Krüger, Z. Phys. **216**, 136 (1968).

[36] R. Ritschel, Z. Phys. **79**, 1 (1932).

[37] I. Mills, T. Cvitas, K. Homann, N. Kallay, and K. Kuchitsu, *Quantities, Units and Symbols in Physical Chemistry* (Blackwell Scientific, Oxford, 1993).